Received: 16 February 2024 | Accepted: 27 May 2024

DOI: 10.1002/prp2.1223

ORIGINAL ARTICLE

A novel and selective fluorescent ligand for the study of adenosine A_{2B} receptors

Foteini Patera[1,2,3] | Sarah J. Mistry[2,4] | Nicholas D. Kindon[2,4] | Eleonora Comeo[2,4] | Joelle Goulding[1,2] | Barrie Kellam[2,4] | Laura E. Kilpatrick[2,4] | Hester Franks[2,3,5] | Stephen J. Hill[1,2]

[1]Division of Physiology, Pharmacology and Neuroscience, School of Life Sciences, University of Nottingham, Nottingham, UK

[2]Centre of Membrane Proteins and Receptors (COMPARE), University of Birmingham and University of Nottingham, Midlands, UK

[3]Centre for Cancer Sciences, School of Medicine, Biodiscovery Institute, University of Nottingham, Nottingham, UK

[4]Division of Biomolecular Science and Medicinal Chemistry, School of Pharmacy, Biodiscovery Institute, University of Nottingham, Nottingham, UK

[5]Department of Oncology, Nottingham University Hospitals NHS Trust, UK

Correspondence
Stephen J. Hill, Division of Physiology, Pharmacology and Neuroscience, School of Life Sciences, University of Nottingham, Nottingham, UK.
Email: stephen.hill@nottingham.ac.uk

Funding information
Medical Research Council, Grant/Award Number: MR/W016176/1; Cancer Research UK, Grant/Award Number: C50808/A24952; Biotechnology and Biological Sciences Research Council, Grant/Award Number: BB/T0083690/1

Abstract

Fluorescent ligands have proved to be powerful tools in the study of G protein-coupled receptors in living cells. Here we have characterized a new fluorescent ligand PSB603-BY630 that has high selectivity for the human adenosine A_{2B} receptor ($A_{2B}R$). The $A_{2B}R$ appears to play an important role in regulating immune responses in the tumor microenvironment. Here we have used PSB603-BY630 to monitor specific binding to $A_{2B}Rs$ in M1- and M2-like macrophages derived from CD14+ human monocytes. PSB603-BY630 bound with high affinity (18.3 nM) to nanoluciferase-tagged $A_{2B}Rs$ stably expressed in HEK293G cells. The ligand exhibited very high selectivity for the $A_{2B}R$ with negligible specific-binding detected at NLuc-$A_{2A}R$, NLuc-A_1R, or NLuc-A_3R receptors at concentrations up to 500 nM. Competition binding studies showed the expected pharmacology at $A_{2B}R$ with the $A_{2B}R$-selective ligands PSB603 and MRS-1706 demonstrating potent inhibition of the specific binding of 50 nM PSB603-BY630 to $A_{2B}R$. Functional studies in HEK293G cells using Glosensor to monitor G_s-coupled cyclic AMP responses indicated that PSB603-BY630 acted as a negative allosteric regular of the agonist responses to BAY 60–6583. Furthermore, flow cytometry analysis confirmed that PSB603-BY630 could be used to selectively label endogenous $A_{2B}Rs$ expressed on human macrophages. This ligand should be an important addition to the library of fluorescent ligands which are selective for the different adenosine receptor subtypes, and will enable study of the role of $A_{2B}Rs$ on immune cells in the tumor microenvironment.

Abbreviations: BODIPY, boron-dipyrromethene; cAMP, cyclic adenosine monophosphate; cDNA, complementary deoxyribonucleic acid; cryo-EM, cryo-electron microscopy; DMEM, Dulbecco's Modified Eagles Medium; EDTA, ethylenediaminetetraacetic acid; ELISA, enzyme linked immuno-absorbent assay; FBS, fetal bovine serum; FCS, fetal calf serum; GMCSF, granulocyte-macrophage colony-stimulating factor; GPCR, G protein coupled receptor; HBSS, Hank's balanced salt solution; HEK293 cells, human embryonic kidney cells; HEPES, 4-(2-hydroxyethyl)-1-piperazineethanesulfonic acid; HPLC, high performance liquid chromatography; IFNγ, interferon γ; IL-10, interleukin 10; IL-12, interleukin 12; LC–MS, liquid chromatography-mass spectrometry; LPS, lipopolysaccharides; MCSF, macrophage colony-stimulating factor; NanoBRET, nanoluciferase bioluminescence resonance energy transfer; NECA, 5-(N-ethylcarboxamido) adenosine; Nluc, nanoluciferase; NMR, Nuclear Magnetic Resonance; PBMC, peripheral blood mononuclear cells; RP-HPLC, reversed phase high performance liquid chromatography; S.E.M., standard error of mean.

FP and SJM contributed equally to this work.

KEYWORDS
adenosine A_{2B} receptor, antagonist, fluorescent ligand, ligand-binding, macrophages, PSB603

1 | INTRODUCTION

Adenosine acts via four different G protein coupled receptor (GPCR) subtypes (A_1R, $A_{2A}R$, $A_{2B}R$ and A_3R).[1,2] A_1R and A_3R primarily couple to $G\alpha_{i/o}$ proteins and inhibit adenylyl cyclase activity, whilst the $A_{2A}R$ preferentially couples to $G\alpha_s$ proteins and stimulates the formation of cyclic AMP (cAMP).[1–4] In contrast, the $A_{2B}R$ appears to be more promiscuous and, as well as coupling to $G\alpha_s$ proteins,[4] there is evidence of coupling of $A_{2B}R$ to other G-proteins, most notably $G\alpha_{q/11}$, $G\alpha_i$ and $G\alpha_{12/13}$ proteins.[5–8] Interestingly, there are differences in the extent to which different $A_{2B}R$ agonists activate different signaling pathways. Thus, adenosine and NECA activate most members of the four Gα protein families ($G\alpha_s$, $G\alpha_{q/11}$, $G\alpha_i$, and $G\alpha_{12/13}$) whilst the A_{2B}-selective partial agonist BAY 60–6583[4,5] preferentially couples to $G\alpha_s$, $G\alpha_{15}$, and $G\alpha_{12}$.[8]

Crystal and/or cryo-electron microscopy (cryo-EM) structures have now been reported for both the $A_{2A}R$ and $A_{2B}R$. The crystal structure of the $A_{2A}R$ has been obtained in antagonist-[9] and agonist-[10,11] bound conformations. A cryo-EM structure is also available for the $A_{2A}R$ coupled to an engineered heterotrimeric G protein.[12] The $A_{2B}R$ is closely related to the $A_{2A}R$, but has low affinity for NECA and adenosine.[3,13] Recently, two $A_{2B}R$ cryo-EM structures co-bound to NECA (PDB: 7XY7) or BAY 60–6583 (PDB: 7XY6) in the presence of an engineered heterotrimeric Gs protein have been published.[14] The overall structure of $A_{2B}R$-NECA-G_s is very similar to that of $A_{2A}R$-NECA.[14] The $A_{2B}R$-BAY60-6583-G_s structure, however, revealed an orthosteric binding pocket similar to that of NECA, but with a secondary binding pocket extending out from the orthosteric binding site where residues $V250^{6.51}$ and $N273^{7.36}$ appear to be key determinants of its selectivity for $A_{2B}R$.[14]

Recent therapeutic interest in $A_{2A}R$ and $A_{2B}R$ has focussed on the role of these Gαs-coupled adenosine receptors on immune cells in relation to cancer progression. For example, activation of $A_{2A}Rs$ on the surface of immune cells can suppress the normal adaptive immune response to the formation of tumors and facilitate cancer growth and tumor cell dissemination.[15–18] This has led to the development of specific $A_{2A}R$ antagonists to inhibit the immunosuppressive effects of $A_{2A}Rs$ in the tumor microenvironment.[19] The $A_{2B}R$ also appears to have a similar role in regulating the immune response in the tumor microenvironment.[20–22] Furthermore, $A_{2B}R$-selective antagonists have been evaluated in patients with non-small cell lung cancer.[20] In addition, tumor-derived exosomes have been shown to promote angiogenesis via $A_{2B}R$ signaling.[23] Thus, these exosomes promote the polarization of macrophages towards an M2-like phenotype and enhance the secretion of angiogenic factors.[23] A key requirement for future studies on the relative role of adenosine receptors in the tumor microenvironment is the need to be able to monitor the expression level of $A_{2A}R$ and $A_{2B}R$ on the surface of individual immune cells. In this context, recent advances in fluorescent ligand technologies have begun to allow the development of live-cell and single cell ligand-receptor binding assays.[24–27]

We have recently described the development of a series of fluorescent antagonist probes for $A_{2A}R$.[28,29] The first series were developed from the $A_{2A}R$-selective antagonist preladenant (SCH420814[30]) and exhibited high affinity and selectivity for $A_{2A}R$ which allowed clear visualization of the receptor location in single living cells using confocal imaging.[28] In a separate strategy, we also designed a fluorescent antagonist based on ZM241385 that incorporated a linker between the pharmacophore and the sulfo-cyanine5 fluorophore (Cy5) that facilitated covalent transfer of the fluorphore to the $A_{2A}R$.[29] This was then used to monitor binding to human macrophages endogenously expressing the $A_{2A}R$.[29] Successful high affinity and A_{2B}-selective fluorescent ligands have also been developed previously (e.g., PSB-12105) using a green-emitting BODIPY fluorophore attached to 8-substituted xanthine derivatives.[31] The aim of the present study was to develop a red-emitting fluorescent antagonist that is selective for $A_{2B}R$. Here we have based our fluorescent probe design on the $A_{2B}R$-selective antagonist PSB603[4,31,32] and demonstrate that it can be used to selectively monitor binding to endogenous adenosine $A_{2B}R$ in human macrophages.

2 | MATERIALS AND METHODS

2.1 | Materials

2-(2-Furanyl)-7-(2-phenylethyl)-7*H*-pyrazolo[4,3-*e*][1,2,4]triazolo[1,5-*c*]pyrimidin-5-amine (Scheme 58261) (Cat# 2270), 2-[[6-Amino-3,5-dicyano-4-[4-(cyclopropylmethoxy)phenyl]-2-pyridinyl]thio]-acetamide (BAY 60–6583) (Cat# 4472), 8-[4-[4-(4-Chlorophenzyl)piperazide-1-sulfonyl phenyl]]-1-propylxanthine (PSB 603) (Cat#3198), *N*-(4-Acetylphenyl)-2-[4-(2,3,6,7-tetrahydro-2,6-dioxo-1,3-dipropyl-1*H*-purin-8-yl)phenoxy]acetamide (MRS 1706) (Cat# 1584), 2-(2-Furanyl)-7-[3-(4-methoxyphenyl)propyl]-7*H*-pyrazolo[4,3-*e*][1,2,4]triazolo[1,5-*c*]pyrimidin-5-amine (Scheme 442416) (Cat#2463), *trans*-4-[(2-Phenyl-7*H*-pyrrolo[2,3-*d*]pyrimidin-4-yl)amino]cyclohexanol (SLV 320) (Cat#3344) and *N*-[9-Chloro-2-(2-furanyl)[1,2,4]-triazolo[1,5-*c*]quinazolin-5-yl]benzene acetamide (MRS 1220) (Cat#1217) were purchased from Tocris Bioscience (Bristol, UK). Dimethyl Sulfoxide (DMSO) (Cat#D5879), lipopolysaccharide (LPS) (Cat# L2654) and Bovine Serum Albumin (BSA) (Cat# A7030) were purchased from Sigma-Aldrich (Gillingham, UK).The cAMP GloSensor™ Human Embryonic Kidney 293 (HEK293G) cell line, the Nano-Glo® Luciferase Assay System and GloSensor™ cAMP reagent were purchased from Promega Corporation (Madison, WI, USA). The human IL-10 DuoSet® (Cat# DY2178), ELISA kit and interferon-γ (Cat# 285-IF-100/CF) were purchased from R&D Systems. The BD OptEIA™

human IL-12 (p70; Cat# 555183) ELISA kit was obtained from BD Biosciences. FuGENE and furimazine were obtained from Promega Corporation (Wisconsin, USA). SNAP-Surface® Alexa Fluor® 488 was obtained from New England Biolabs (Hitchin, UK). All other chemicals were from Sigma-Aldrich (Missouri, USA). Nunc™ Lab-tek™ chambered coverglass (155361) were obtained from Thermo Fisher Scientific (Paisley, UK). 96-well white clear-bottomed plates and 35 mm Cellview 4-quadrant culture dishes were from Greiner bio-one (Kremsmunster, Austria). The synthesis of the fluorescent ligands AV039 (compound 19 in[33]), EC069 (compound 44b in[34]) and EC005 (compound 12 in[22]) have been described previously.

2.2 | Chemistry

Chemicals and solvents of analytical and HPLC grade were purchased from commercial suppliers and used without further purification. BODIPY-630/650-X-SE was purchased from Molecular Probes (Thermo Fisher Scientific). All reactions were carried out at ambient temperature unless otherwise stated. Reactions were monitored by thin-layer chromatography on commercially available silica pre-coated aluminium-backed plates (Merck Kieselgel 60 F254). Visualization was under UV light (254 nm and 366 nm), followed by staining with ninhydrin or $KMnO_4$ dips. Flash column chromatography was performed using silica gel 60, 230–400 mesh particle size (Sigma Aldrich). NMR spectra were recorded on a Bruker-AV 400. ^{1}H spectra were recorded at 400.13 Hz and ^{13}C NMR spectra at 101.62 Hz. All ^{13}C NMR are ^{1}H broadband decoupled. Solvents used for NMR analysis (reference peaks listed) were $CDCl_3$ supplied by Cambridge Isotope Laboratories Inc., (δ_H = 7.26 ppm, δ_C = 77.16) and CD_3OD supplied by VWR (δ_H = 3.31 ppm and δ_C = 49.00). Chemical shifts (δ) are recorded in parts per million (ppm) and coupling constants are recorded in Hz. The following abbreviations are used to described signal shapes and multiplicities; singlet (s), doublet (d), triplet (t), quadruplet (q), broad (br), dd (doublet of doublets), ddd (double doublet of doublets), dtd (double triplet of doublets) and multiplet (m). Spectra were assigned using appropriate COSY and HSQC experiments. Processing of the NMR data was carried out using the NMR software Topspin 3.0. LC–MS spectra were recorded on a Shimadzu UFLCXR system coupled to an Applied Biosystems API2000 and visualized at 254 nm (channel 1) and 220 nm (channel 2). LC–MS was carried out using a Phenomenex Gemini-NX C18 110A, column (50 mm × 2 mm × 3 μm) at a flow rate 0.5 mL/min over a 5 min period. All high resolution mass spectra (HRMS) were recorded on a Bruker microTOF mass spectrometer using MS electrospray ionization operating in positive ion mode. RP-HPLC was performed on a Waters 515 LC system and monitored using a Waters 996 photodiode array detector at wavelengths between 190 and 800 nm. Spectra were analyzed using Millenium 32 software. Semi-preparative HPLC was performed using YMC-Pack C8 column (150 mm × 10 mm × 5 μm) at a flow rate of 5.0 mL/min using a gradient method of 40%–95% B over 15 min (Solvent A = 0.01% formic acid in H_2O, solvent B = 0.01% formic acid in CH_3CN (method A)) or 40%–75% B over 10 min (Solvent A = 0.01% formic acid in H_2O, solvent B = 0.01% formic acid in CH_3CN (method B)). Analytical RP-HPLC was performed using a YMC-Pack C8 column (150 mm × 4.6 mm × 5 μm) at a flow rate of 1.0 mL/min. Final products were one single peak and >95% pure. The retention time of the final product is reported using a gradient method of 5%–95% solvent B in solvent A over 25 min. (Solvent A = 0.01%) formic acid in H_2O, (solvent B = 0.01%) formic acid in CH_3CN. Full experimental detail for the synthesis of PSB603-BY630 (Figure 1) can be found in the Supplementary Information.

2.3 | Cell lines

HEK293T cells were obtained from ATCC (Virginia, USA). A clonal HEK 293 cell line stably expressing the cAMP GloSensor (20F) biosensor (HEK293G)[4,35] was obtained from Promega Corporation (Madison, WI, USA). HEK293T and HEK293G cell lines were maintained in Dulbecco's Modified Eagles Medium (DMEM; Sigma-Aldrich, Missouri USA) supplemented with 10% fetal bovine serum (FBS; Sigma-Aldrich, Missouri USA) at 37°C 5% CO_2. The generation of HEK293T or HEK293G cells stably expressing NanoLuc-A_1R, NanoLuc-A_{2B}R and NanoLuc-A_3R have been described previously.[28,36]

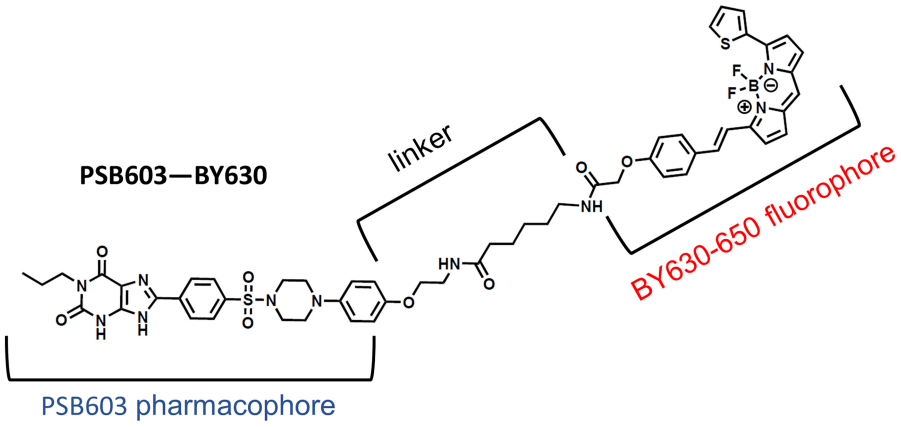

FIGURE 1 Structure of PSB603-BY630.

2.4 | Transient expression of NanoLuc-A_{2A}R

The human A_{2A} receptor cDNA was obtained from Missouri S&T cDNA Resource Centre (www.cdna.org) in a pcDNA3.1 expression vector. An N-terminal nanoluciferase (NLuc)-labeled human A_{2A}R receptor constructs (NLuc-A_{2A}R) was then generated in frame with the full length NLuc incorporating a rat 5-HT_{3A} membrane localisation signal sequence in pcDNA3.1 as described previously.[37] For transient transfections, HEK293G cells were seeded at 20000 cells/well into white walled, clear bottomed 96-wells plates (Greiner Bio-One, Stonehouse, UK), coated with 10 μg/mL poly-D-lysine, in 100 μL medium/well and incubated at 37°C and 5% CO_2 for 18–24 h. After 24 h, cells were transfected with 100 ng per well of pcDNA3.1 NLuc-A_{2A}R diluted in Opti-MEM, using FuGENE HD at a 3:1 reagent to DNA ratio following manufacturer's instructions. Following a 10 min incubation at room temperature, 5 μL per well of transfection mix was added to each well. Cells were left at 37°C 5% CO_2, for 24 h prior to NanoBRET assays.

2.5 | NanoBRET binding assay

Saturation and competition binding assays were performed as previously described.[36] Briefly, cells were seeded in 96-well white clear-bottomed Greiner plates pre-treated with 10 μg/mL poly-D-lysine (Sigma-Aldrich, Missouri USA) at a density of 30000–35000 cells per well in DMEM supplemented with 10% FBS. The following day medium was removed and cells were incubated with PSB603-BY630 in the presence or absence of 1 μM MRS1706 (saturation binding assays) or competing ligand in the presence of 50 nM PSB603-BY630 (competition binding assays) in HEPES buffered saline solution (HBSS; 145 mM NaCl, 5 mM KCl, 1.3 mM $CaCl_2$, 1 mM $MgSO_4$, 10 mM HEPES, 2 mM sodium pyruvate, 1.5 mM $NaHCO_3$, 10 mM D-glucose, pH 7.45) with 0.1% bovine serum albumin for 1 h at 37°C. The NanoLuc substrate, furimazine (Promega Corporation, Wisconsin, USA), was then added to each well (1:400 dilution) and the plate was incubated for 10 min in the dark at 37°C. The resulting bioluminescence resonance energy transfer (BRET) was measured using a PHERAstar FS plate reader (BMG Labtech) at 37°C. For each well, filtered light emissions at 460 nm (80 nm bandpass) and >610 nm (longpass) for the BODIPY630/650 ligand were simultaneously measured. BRET ratios were calculated by dividing the 610 nm emission by the 460 nm emission. All conditions were performed in 2–6 replicates within each plate. For kinetic experiments, cells were preincubated for 10 min with 1:400 dilution of furimazine prior to addition of 200 nM PSB603-BY630 and BRET ratios determined every 0.5 min. At 60 min, 10 μM MRS-1706 was added and the ligand-binding kinetics followed for a further 60 min.

2.6 | cAMP GloSensor™ luminescence assay

The cAMP GloSensor™ luminescence assay was performed according to the manufacturer's instructions (Promega Corporation, Madison, WI, USA). Briefly, after 24 h incubation at 37°C and 5% CO_2 after cell plating (40000 cells/well in 100 μL), medium was aspirated from each well of the 96-well plate. Cells were incubated in 50 μL HEPES buffered saline solution (HBSS; 2 mM sodium pyruvate, 145 mM NaCl, 10 mM D-glucose, 5 mM KCl, 1 mM $MgSO_4.7H_2O$, 10 mM HEPES, 1.3 mM $CaCl_2$, 1.5 mM $NaHCO_3$ in double-distilled water, pH 7.45) containing 3% GloSensor™ cAMP reagent at 37°C for 1.5 h. For agonist studies, an initial baseline luminescence read was made at time zero, the plate was then removed from the plate-reader and a further 50 μL HBSS containing agonist (2× final concentration) or HBSS (vehicle control) added. Luminescence was measured on an open channel (gain of 3600) immediately after these additions, and then continuously over 60 min, reading each well once every minute, by a PHERAstar FSX microplate reader (BMG Labtech, Offenburg, Germany) at 37°C. Increases in luminescence are indicative of intracellular cAMP accumulation, thus the temporal changes in relative cytosolic cAMP concentration were measured upon agonist or vehicle addition. Antagonist action was determined following 30 min pre-incubation of HBSS in the presence of 20 and 200 nM PSB603-BY630 and read as above. All conditions were performed in triplicates within each plate.

2.7 | NanoBRET imaging

Cells were seeded onto 35 mm Cellview 4-quadrant culture dishes (Greiner Bio-one), which have a 10 mm glass coverslip bottom, in DMEM supplemented with 10% FBS at a density of 100000 cells per quadrant 2 days prior to experiment in total volume of 500 μL. On the day of the experiment medium was replaced with HBSS in the presence or absence of PSB603-BY630 (100 nM) and/or MRS1706 (10 μM) and incubated for 30 min at 37°C before imaging. Bioluminescence and NanoBRET imaging were performed on an Olympus LuminoView 200 microscope with a 60× NA1.42 oil immersion objective with a 0.5× tube lens, following addition of furimazine (1:800 dilution) (Promega). Images were captured by a C9100-23B IMAGE EMX2 camera (Hamamatsu, Japan) with gain set at 200 for all channels. Filtered bioluminescence was captured using a 438/24 bandpass filter, BRET in the presence of PSB603-BY630 was captured using a 650/50 nm bandpass filter. For the NLuc-A_{2B}R stable cell line exposure times were set at 10 s for filtered bioluminescence and 75 sec for BRET. Raw intensity values were determined for three regions of interest per experiment per condition and the BRET ratio calculated by dividing the raw intensity recorded from the BRET capture by the filtered bioluminescence capture. Corrected BRET ratios were determined by subtracting the BRET ratio determined from a control quadrant (HBSS alone). For each condition five separate experiments were performed.

2.8 | Human macrophage generation

One hundred and fifty milliliter peripheral blood was obtained in heparinised 60 mL syringes by venepuncture from healthy volunteers after written informed consent (Ethics from University of

Nottingham Ethics committee, ref 161–1711). Peripheral blood mononuclear cells (PBMC) were immediately separated by density centrifugation over Lymphoprep (Stemcell, UK) at 800*g* for 25 min on low brake followed by washes in endotoxin-free phosphate-buffered saline (PBS, Sigma). PBMC were washed in MACS buffer (PBS + 1% fetal calf serum (FCS, Sigma) + 2 μM EDTA (Sigma)) then incubated with CD14 microbeads (Miltenyi Biotech) and monocytes isolated by magnetic separation on an AutoMACS Pro cell separator (Miltenyi). Cell purity was routinely assessed by flow cytometry (>95%). Purified CD14+ monocytes were differentiated into macrophages at 37°C/5% CO_2 for 7 days at 1×10^6/well in low-attachment 24-well plates (Corning Costar) in 1 mL macrophage medium (RPMI 1640 (Sigma) supplemented with 10% endotoxin-free FCS (Sigma) and 1% sodium pyruvate (Sigma)) plus cytokines. For M1-like macrophages, Granulocyte-macrophage colony-stimulating factor (GMCSF, Peprotech) was added at day 0 at 20 U/mL and for M2-like macrophages, Macrophage colony-stimulating factor (MCSF, Immunotools) at 10 ng/mL. Culture medium was supplemented at day 4 with equal volume of medium + GMCSF or MCSF as appropriate. Macrophage phenotype validation was confirmed based on morphological observation using a Nikon ECLIPSE TS100 inverted microscope in 20X magnification and by cytokine secretion profile with M1-like macrophages secreting high IL-12 and low IL-10, and M2-like macrophages secreting low IL-12 and high IL-10.

2.9 | ELISA analysis of IL-12 and IL-10 secretion from M1- and M2- like human macrophages in response to stimulation as phenotypic confirmation

Following differentiation of CD14+ monocytes for 7 days with either GMCSF (for M1-like macrophages) or MCSF (for M2-like macrophages) as described above, M1- and M2-like macrophages were dislodged from plates by incubation on ice for 25 min in cold endotoxin-free PBS. Harvested macrophages were used for labelling and flow cytometry (see 2.10) and separately seeded at a density 5×10^4 cells/well in a total volume of 100 μL of macrophage medium in a standard 96 well plate (ThermoFisher) for cytokine stimulation as a phenotypic readout. After resting for 2 h at 37°C/5% CO_2, 100 μL of medium containing either LPS (1 mg/mL) plus interferon-γ (IFNγ; 1000 U/mL) for M1-macrophages or LPS (1 mg/mL) alone for M2-like macrophages was added. Supernatants were collected from triplicate wells after a 24 h incubation at 37°C/5% CO_2. A single well of unstimulated cells was run as negative control per macrophage type. The levels of IL-10 or IL-12 cytokines were determined using the Human IL-10 DuoSet® or the BD OptEIA™ Human IL-12 (p70) ELISA kits respectively according to manufacturers' instructions.

2.10 | Macrophage labelling and flow cytometry

Harvested macrophages were resuspended in staining buffer (HBSS [Sigma] supplemented with 2.5% v/v FCS and Ethylenediaminetetraacetic acid- EDTA 5 mM) at 2×10^6 cells/mL. Samples of 2×10^5 cells in 200 μL were incubated with 100 nM PSB603-BY630 for 20 min at RT with or without a 30 min RT pre-incubation with 10 μM PSB603. BODIPY 630/650 fluorescence was measured on a MACSQuant 10 Flow Cytometer (Miltenyi) immediately after incubation (>5×10^4 events acquired). Flow cytometry data were analyzed using FlowJo software v10. The gating strategy used for the flow cytometry experiments is provided in the Supplementary Information.

2.11 | Data analysis

Data were analyzed using Prism 7.4 software (GraphPad, San Diego, USA). Saturation NanoBRET curves were fitted simultaneously for total (PSB603-BY630) and non-specific binding (in the presence of 10 μM MRS1706) using the following equation:

$$\text{Total binding} = \frac{B_{max} \times [B]}{[B] + K_D} + m \times B + c$$

where B_{max} is the maximal specific binding, [*B*] is the concentration of the fluorescent ligand (nM), K_D is the equilibrium dissociation constant (nM), *m* is the slope of the non-specific binding component, and *C* is the y-axis intercept.

The affinities of ligands at the NLuc-A_{2A}R were calculated from competition binding data with a one-site sigmoidal response curve given by the following equation:

$$\%\text{Inhibition of specific binding} = \frac{(100 \times [A^n])}{([A^n] + IC_{50}^n)}$$

where [A] is the concentration of unlabelled ligand, *n* is the Hill coefficient, and IC_{50} is the concentration of ligand required to inhibit 50% of fluorescent ligand. The IC_{50} values were then used to calculate the K_i values using the Cheng-Prussoff equation:

$$K_i = \frac{IC_{50}}{1 + \frac{[L]}{K_D}}$$

where [*L*] is the concentration of PSB603-BY630 in nM, and K_D is the dissociation constant of that fluorescent ligand in nM.

Bioluminescence and NanoBRET images were analyzed using ImageJ (http://rsb.info.nih.gov/ij; NIH, USA) and the Time Series Analyzer version 3.0 (https://imagej.nih.gov/ij/plugins/time-series.html).[38]

For kinetic binding experiments, the BRET ratio obtained in the absence of fluorescent ligand was determined for each time point and subtracted from the total binding to obtain baseline-corrected values for total binding at each time point. 60 min after addition of 200 nM PSB603-BY630, 10 μM MRS-1706 was added and the dissociation data fitted to the following equation to obtain values for the dissociation rate constant (k_{off}) in min^{-1}:

$$Y = (Yo - NS).e^{-k_{off}.t} + NS$$

where [Yo] is the binding at time 60 min (when 10 μM MRS-1706 was added), NS is the non-specific binding at infinite time, k_{off} is dissociation rate constant. The residence time in min was then calculated as the reciprocal of k_{off}.

2.12 | Nomenclature of targets and ligands

Key protein targets and ligands in this article are hyperlinked to corresponding entries in http://www.guidetopharmacology.org, the common portal for data from the IUPHAR/BPS Guide to PHARMACOLOGY,[39] and are permanently archived in the Concise Guide to PHARMACOLOGY 2019/20.[40]

3 | RESULTS

3.1 | Synthesis of PSB603-BY630

Development of the fluorescent ligand PSB603-BY630 (Figure 1) was based on the $A_{2B}R$ selective xanthine-based ligand PSB-603 which displays sub-nanomolar affinity for $A_{2B}R$ and has a large selectivity over the other adenosine receptor family subtypes (A_1, A_{2A} and A_3).[4,32] A fluorescent ligand generally consists of a targeting binding moiety, linker and fluorophore (Figure 1), and it is essential to take into account the properties of each of these components as each of them can affect the overall affinity and selectivity of the final fluorescent ligand.[41,42] BODIPY 630/650-X was selected as the fluorophore moiety, due to its excellent optical properties and established use in the development of a toolbox of subtype-selective fluorescent ligands for the family of the adenosine receptors.[28,33,34] A previous structure–activity relationship (SAR) study of PSB-603 analogues indicated that para-substitution of the terminal aromatic ring, with lipophilic substituents, is well tolerated.[43] Correspondingly, we sought to extend from this position via an aminoethyl handle which enabled us to directly attach the BODIPY 630/650-X fluorophore (Figure 1). The synthesis of this fluorescent ligand is detailed in Supplementary Information (Figure S1).

3.2 | Pharmacological characterization of PSB603-BY630 binding to $A_{2B}R$

An initial assessment of the binding of PSB603-BY630 to human $A_{2B}Rs$ was made using NanoBRET in live HEK293G cells stably expressing $A_{2B}Rs$ tagged with an N-terminal nanoluciferase (NLuc-$A_{2B}R$) (Figure 2). Clear saturable binding was detected at concentrations up to 500 nM that was prevented by simultaneous incubation with the $A_{2B}R$-selective inverse agonist MRS-1706 (1 μM; Figure 2A). The mean *KD* value determined in five separate experiments for the

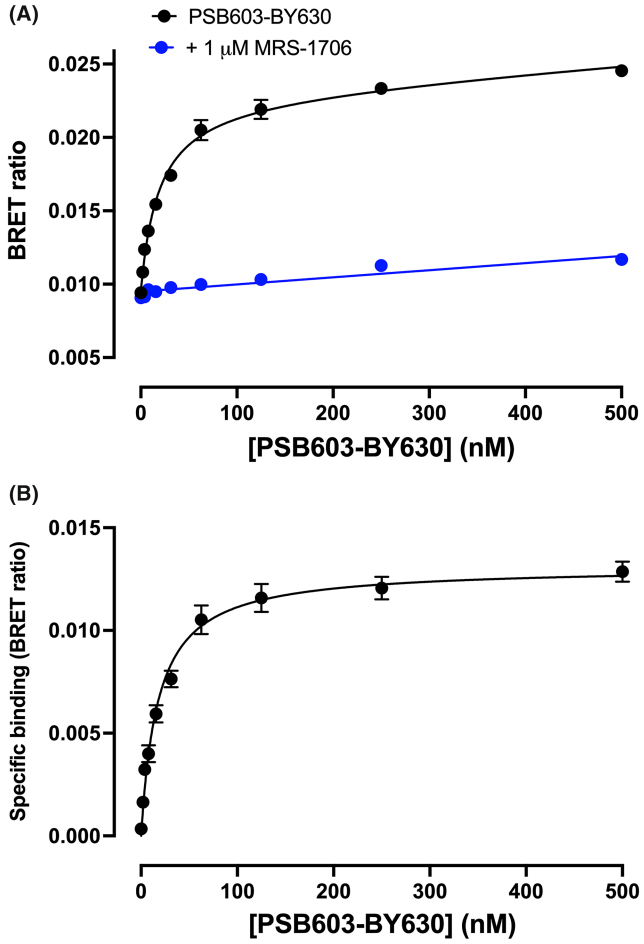

FIGURE 2 NanoBRET binding curves for PSB603-BY630 in HEK293G cells exogenously expressing NLuc-$A_{2B}R$. (A) Cells were incubated with increasing concentrations of PSB603-BY630 in the absence or presence of 1 μM MRS-1706. (B) Specific-binding of PSB603-BY630 to NLuc-$A_{2B}Rs$. Data are mean ± S.E.M obtained in five independent experiments (each conducted in triplicate). The mean K_D value obtained in five separate experiments was 18.32 ± 1.65 nM.

specific component of binding (Figure 2B) was 18.32 ± 1.65 nM. This value was of a similar magnitude to that (3.6 nM) determined for [^{3}H]-PSB603 binding to membranes from CHO cells expressing the human $A_{2B}R$.[13]

Plate reader-based saturable binding of PSB603-BY630 monitored using NanoBRET in cell populations does not give, however, any indication of the subcellular location of the ligand-receptor interaction in intact cells. To gain some insight into cellular location we also monitored the binding of PSB603-BY630 to membrane-bound $A_{2B}Rs$ in individual cells using bioluminescence imaging (Figure 3). In these experiments cells were incubated with 100 nM PSB603-BY630 in the absence and presence of 10 μM MRS-1706 for 30 min before addition of furimazine (1:800 dilution) and subsequent imaging. Filtered bioluminescence was captured for 10 s using a 438/24 bandpass filter in order to detect the location of the nanoluciferase-tagged $A_{2B}Rs$ (cyan in Figure 3A,C). It is clear that there is substantial expression of the NLuc-$A_{2B}R$ at the cell surface. A longer integration

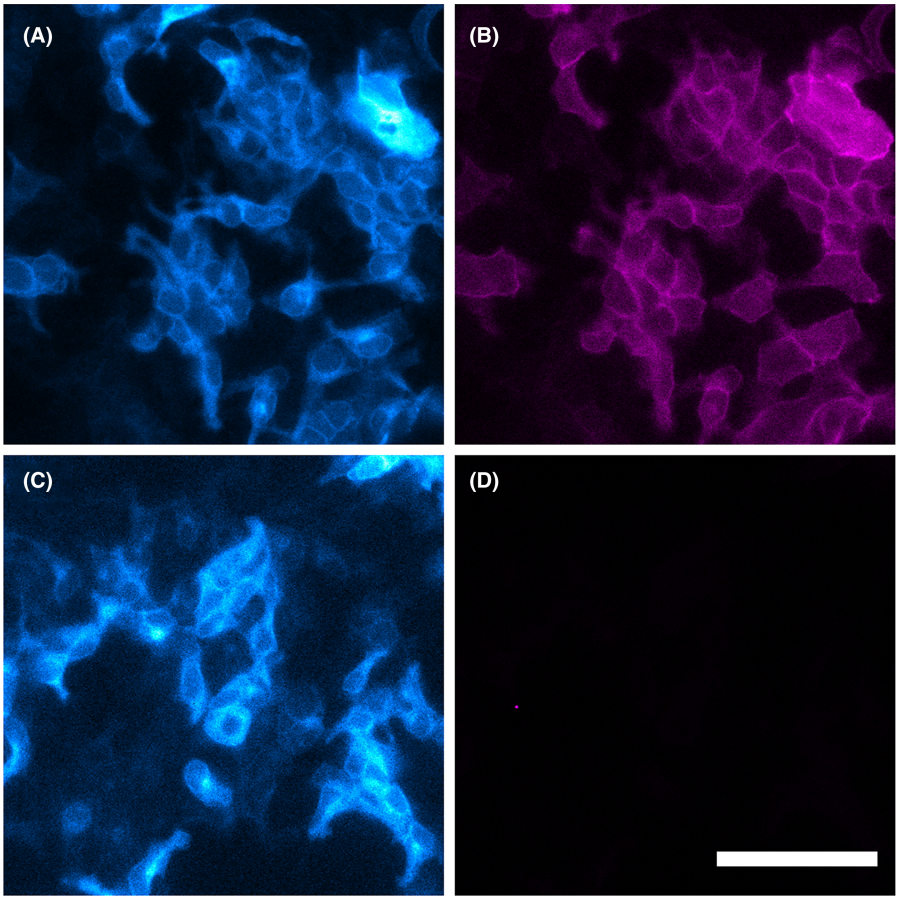

FIGURE 3 NanoBRET imaging of PSB603-BY630 binding to HEK293G cells expressing NLuc-A_{2B}R. Cells were incubated with 100 nM PSB603-BY630 in the absence (A, B) or presence (C, D) of 10 μM MRS-1706 before addition of furimazine (1:800 dilution) and imaging. Filtered bioluminescence was captured using a 438/24 bandpass filter (cyan A & C). BRET was captured using a 650/50 nm bandpass filter (magenta B & D). Images are representative of those obtained in five independent experiments. Scale bar represents 100 μm.

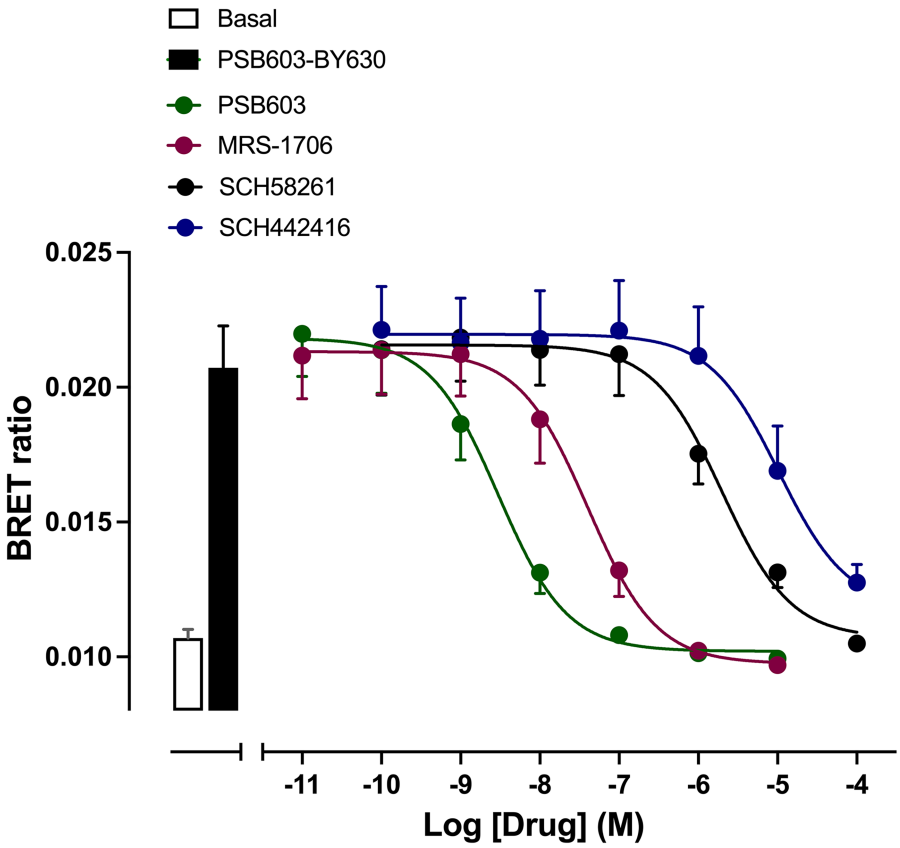

FIGURE 4 NanoBRET competition binding in HEK293G cells exogenously expressing NLuc-A_{2B}R. Cells were incubated with 50 nM PSB603-BY630 in the absence or presence of competing ligands Data are mean ± S.E.M. from five independent experiments. The open and closed bars show the BRET ratio obtained in the absence and presence of 50 nM PSB603-BY630 respectively.

time (75 s) was used to monitor the ligand-binding BRET signal using a 650/50 nm bandpass filter (magenta in Figure 3B,D). This showed clear binding to cell surface receptors that can be completely prevented by co-incubation with the A_{2B}R-selective inverse agonist MRS-1706 (Figure 3B,D).

Competition binding experiments demonstrated that the binding of 50 nM PSB603-BY630 could be inhibited by a panel of different adenosine receptor-selective ligands (Figure 4; Table 1) with an appropriate pharmacology for binding selectively to the A_{2B}R. The most potent inhibitors were the A_{2B}R antagonist PSB603[4,32] and the A_{2B}R selective inverse agonist MRS-1706.[44] In contrast, the selective A_{2A}R-antagonists SCH442416 and SCH58261,[45,46] the A_1R-selective antagonist SLV320[34] and the A_3R-selective antagonist MSR1220[32] were much weaker (Figure 4; Table 1).

Ligand-binding kinetics of 200 nM PSB603-BY630 indicated that equilibrium was achieved within 60 min at 37°C (Figure 5). At 60 min, 10 μM MRS-1706 was then added to initiate fluorescent ligand dissociation (Figure 5). Fitting a single exponential function to these data allowed the dissociation rate constant k_{off} to be determined. This yielded a mean value of 0.065 ± 0.003 min^{-1} for k_{off} in 5 independent experiments. This equates to an average residence time of the fluorescent ligand of 15.4 min.

TABLE 1 Log IC_{50} and apparent log K_i values for inhibition of the binding of 50 nM PSB603-BY630 obtained in five separate experiments.

Competitor	Log IC_{50}	Appararent Log K_i	*n*
PSB603	−8.55 ± 0.08	−9.12 ± 0.08	5
MRS1706	−7.44 ± 0.09	−8.01 ± 0.09	5
SCH442416	−5.02 ± 0.14	−5.59 ± 0.14	5
SCH58261	−5.68 ± 0.09	−6.26 ± 0.09	5
SLV320	−5.19 ± 0.18	−5.76 ± 0.18	5
MRS1220	−5.82 ± 0.19	−6.40 ± 0.19	5

Note: Values show mean ± S.E.M. Apparent log K_i values were calculated from IC_{50} values on the assumption that there is a competition between the inhibitor and PSB603-BY630 for the same binding site.

3.3 | Receptor selectivity of PSB603-BY630

To investigate the receptor selectivity of PS603-BY630, we undertook saturation binding experiments in HEK293G cells transiently transfected with the human NLuc-A_{2A}R (Figure 6A), a stable HEK293T cell line expressing the human NLuc-A_1R (Figure 6C) or a stable HEK293G cell expressing the human NLuc-A_3R (Figure 6E). At concentrations up to 500 nM, PSB603-BY630 showed negligible specific binding to NLuc-A_{2A}R, NLuc-A_1R or NLuc-A_3R (Figure 6). In marked contrast, high affinity specific binding was detected in parallel experiments on each receptor with receptor-selective fluorescent ligands for A_{2A}R (EC005[22];

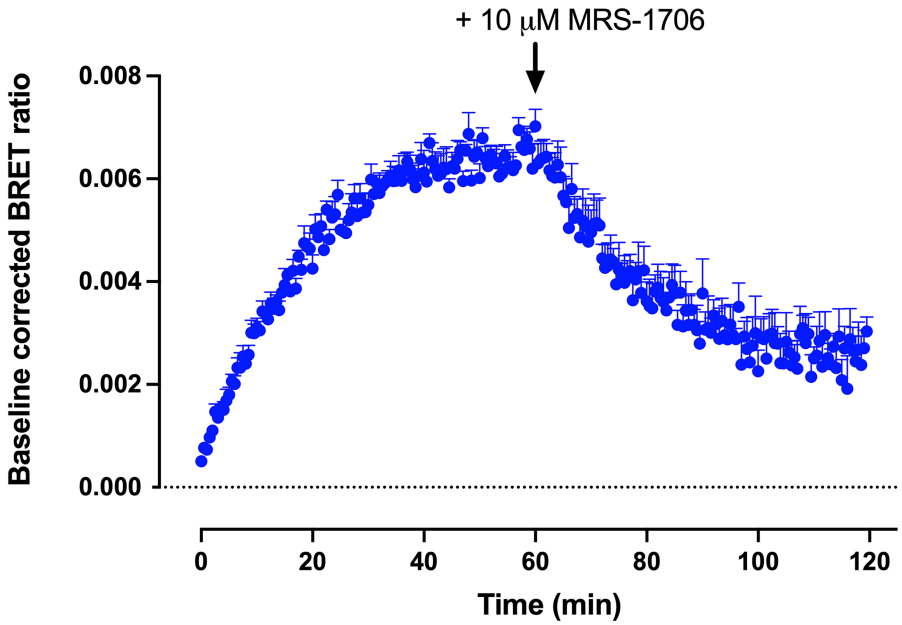

FIGURE 5 Ligand-binding kinetics of 200 nM PSB603-BY630 in HEK293G cells exogenously expressing NLuc-A_{2B}R. BRET ratios for the total binding of 200 nM PSB603-BY630 were obtained every 30 sec. In parallel, data were also collected in the absence of fluorescent ligand for each time point and these data were subtracted from the total binding to obtain baseline-corrected values for total binding at each time point. Sixty minutes after addition of 200 nM PSB603-BY630, 10 μM MRS-1706 was added to initial dissociation of the fluorescent ligand. Values show mean ± S.E.M of quadruplicate determinations in a single representative experiment. Similar data were obtained in four other experiments. The data points for the dissociation phase of the experiment were then fitted to a single exponential function to determine the the dissociation rate constant (k_{off}) in min^{-1} as described under Methods. In this representative experiment the calculated K_{off} value was 0.056 min^{-1}. The mean K_{off} value obtained in the five repeat experiments was 0.065 ± 0.003 min^{-1}.

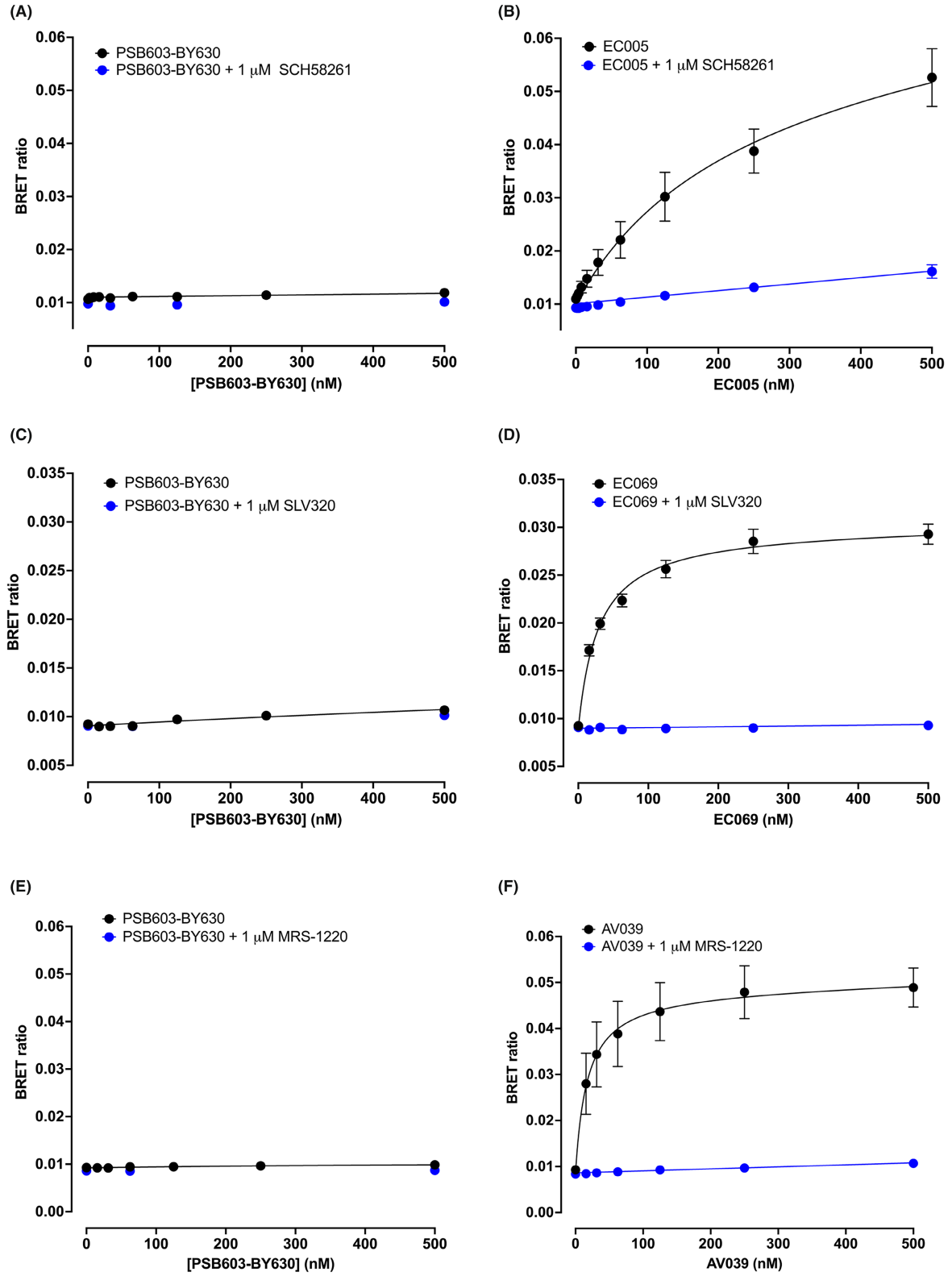

FIGURE 6 NanoBRET binding curves for PSB603-BY630 and receptor-selective fluorescent ligands binding to NLuc-tagged A_1, A_{2A} or A_3 adenosine receptors. (A, B) Total and non-specific binding of (A) PSB603-BY630 or (B) EC-005 to transiently transfected NLuc-A_{2A}R obtained in the absence and presence of 1 μM of the A_{2A}R-selective antagonist SCH58261. Data are mean ± S.E.M obtained in five independent experiments (each conducted in duplicate). (C, D) Total and non-specific binding of (C) PSB603-BY630 or (D) EC-069 to NLuc-A_1R in a stable HEK293T cell line obtained in the absence and presence of 1 μM of the A_1R-selective antagonist SLV320. Data are mean ± S.E.M obtained in five independent experiments (each conducted in triplicate). (E, F) Total and non-specific binding of (E) PSB603-BY630 or (F) AV-039 to NLuc-A_3R in a stable HEK293G cell line obtained in the absence and presence of 1 μM of the A_3R-selective antagonist MRS-1220. Data are mean ± S.E.M obtained in five independent experiments (each conducted in triplicate).

Figure 6B), A_1R (EC069[34]; Figure 6D) and A_3R (AV039[33]; Figure 6F), respectively.

3.4 | Functional cAMP responses in HEK293G cells endogenously expressing $A_{2B}Rs$

HEK293G cells that express the cAMP biosensor Glosensor also endogenously express both $A_{2B}R$ and $A_{2A}R$.[4] These cells therefore provide an opportunity to evaluate the pharmacological characteristics of PSB603-BY630 in cells that express endogenous and untagged $A_{2B}Rs$. We have previously shown that the A_{2B}-selective agonist BAY 60–6583 can elicit selective $A_{2B}R$-mediated Glosensor responses in these cells.[4] Here we show that 20 nM and 200 nM PSB603-BY630 produces a marked and significant ($p<.01$ and $p<.0001$ respectively; two way ANOVA) concentration-dependent reduction in the maximal response to BAY 60–6583 without altering the EC_{50} of the $A_{2B}R$ agonist (Figure 7A; Table 2). These data are very similar to those reported previously for non-fluorescent PSB603.[4] Furthermore, in a stable cell line overexpressing human NLuc-$A_{2B}Rs$, the EC_{50} values for BAY 60–6583 were shifted to lower agonist concentrations consistent with an increase in the spare receptor reserve caused by $A_{2B}R$ overexpression (Figure 7B; Table 2). In these cells 20 nM and 200 nM PSB603-BY630 produced a small increase in the EC_{50} for BAY 60–6583 (Table 2) that was accompanied by a significant decrease in the maximal response to BAY 60–6583 ($p<0.001$ and $p<0.0001$ respectively; two way ANOVA; Figure 7B; Table 2).

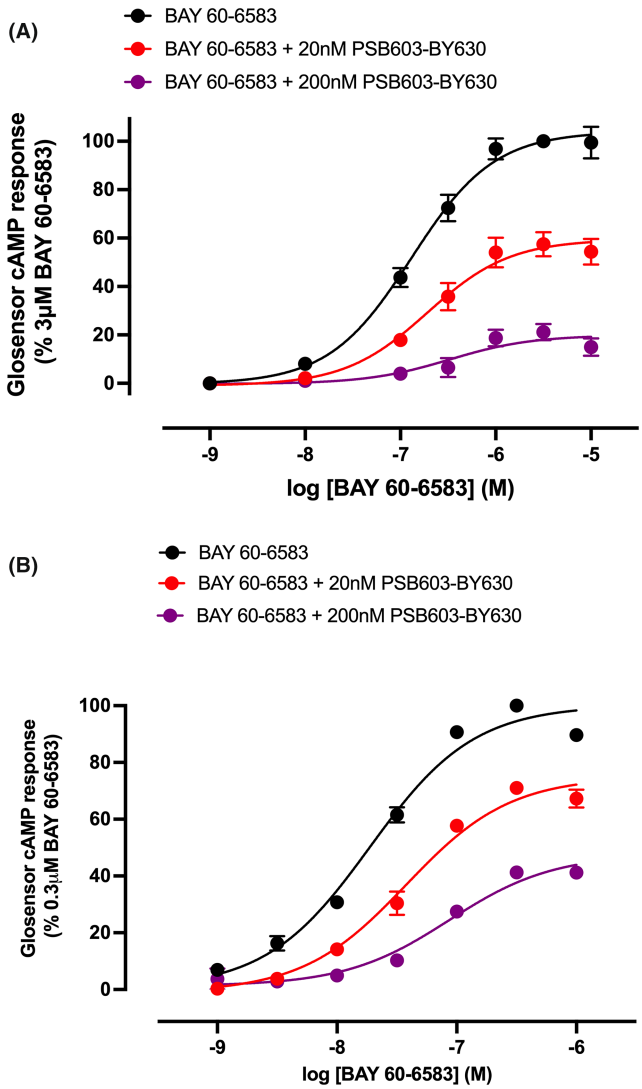

FIGURE 7 Effect of PSB603-BY630 on Glosensor cAMP concentration-response curves to the A_{2B}-selective agonist BAY 60–6583 in (A) HEK293G cells endogenously expressing $A_{2B}R$ or (B) HEK293G cells overexpressing NLuc-$A_{2B}R$. Concentration response curves were obtained in the absence and presence of 20 nM or 200 nM PSB603-BY630. Values are mean ± S.E.M. of five separate experiments carried out in triplicate. Data represent peak luminescence response and are expressed as a percentage of the peak luminescence response to 3 μM BAY 60–6583 (in a) or 0.3 μM BAY 60–6583 (in b) obtained in the absence of antagonist in each individual experiment.

3.5 | PSB603-BY630 binding to human M1-like and M2-like macrophages

To evaluate the potential of this fluorescent ligand to monitor endogenous $A_{2B}R$ expression on human macrophages, we used flow cytometry to monitor specific PSB603-BY630 binding in M1-like and M2-like macrophages. M1-like and M2-like macrophages were prepared from CD14+ human monocytes by differentiation (7 days) in macrophage medium containing GMCSF (20 U/mL) or MCSF (10 ng/mL) respectively. Macrophages were then labeled for 20 min (at room temperature) with 100 nM PSB603-BY630 (in the presence or absence of 10 μM unlabelled PSB603) before being subjected to flow cytometry. Analysis of forward and side light scattering was used to gate out debris and exclude macrophage doublets (Figures S2,S3). Populations of singlet macrophages were then analyzed to generate histograms of cell count versus PSB603-BY630 fluorescence intensity for M1-like (Figure 8A) and M2-like (Figure 8C) macrophages. Median fluorescence intensities obtained in M1-like and M2-like macrophages prepared from six independent donors are shown in Figure 8B,D respectively. Data from each donor were obtained in the presence and absence of unlabelled PSB603 (10 μM) and each symbol represents paired macrophages from a single donor. In both macrophage populations there was a significant inhibiton of PSB603-BY630 binding by inclusion of 10 μM PSB603 to define non specific binding ($p<.01$; paired *t*-test).

4 | DISCUSSION

The present study reports on the properties of a new and selective red-emitting fluorescent ligand (PSB603-BY630) for the human $A_{2B}R$. This molecule, together with the previously reported green-emitting PSB-12105,[31] makes a good addition to existing fluorescent ligands which are selective for the $A_{2A}R$[28,29] and opens the

TABLE 2 Log EC_{50} and E_{MAX} values obtained in HEK293G cells endogenously expressing $A_{2B}R$ or HEK293G cells expressing recombinant human $A_{2B}R$ for BAY 60–6593 obtained in the absence and presence of increasing concentrations of PSB603BY630.

Agonist treatment	Endogenous HEK293G Log EC_{50}	Endogenous HEK293G E_{MAX} (% of response to 3 μM BAY-60-6583)	*n*	HEK293G $A_{2B}AR$ Log EC_{50}	HEK293G $A_{2B}AR$ E_{MAX} (% of response to 0.3 μM BAY-60-6583)	*n*
BY 60–6583	−6.89 ± 0.06	104.15 ± 3.09	5	−7.73 ± 0.03	100.2 ± 1.29	5
BY 60–6583 + 20 nM PSB603-BY630	−6.71 ± 0.10	59.98 ± 5.76**	5	−7.43 ± 0.07*	75.13 ± 2.48***	5
BY 60–6583 + 200 nM PSB603-BY630	−6.51 ± 0.16	20.63 ± 3.54****	5	−7.06 ± 0.03***	47.67 ± 0.86****	5

Note: E_{MAX} values are expressed as a percentage of the response obtained with 3 μM BAY 60–6583 or 0.3 μM BAY 60–6583 in cells recombinant expressing $A_{2B}R$. Significant differences to that seen in the absence of antagonist are indicated (*$p<.05$, ** $p<.01$, *** $p<.001$ or ****$p<.0001$, 2-way ANOVA with Dunnett's multiple comparison test). Data are expressed as mean ± S.E.M. of 5 separate experiments.

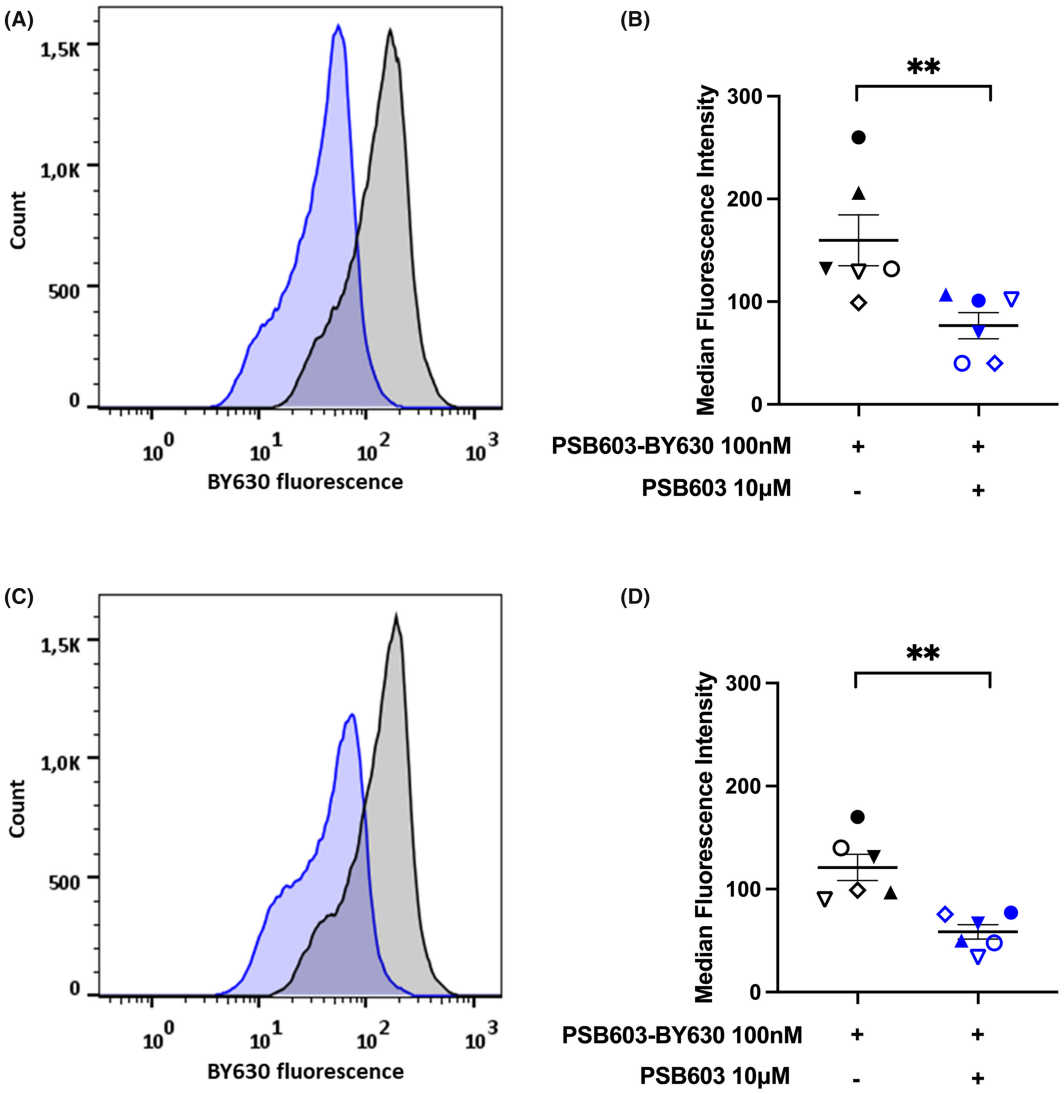

FIGURE 8 Flow cytometry data for the binding of 100 nM PSB603-BY630 to endogenous $A_{2B}R$ in human monocyte-derived M1-like or M2-like macrophages. (A) Flow cytometry histograms obtained in the absence and presence of the A_{2B}-selective antagonist PSB603 in a representative experiment from M1-like macrophages differentiated from monocytes from a single representative donor. (B) Mean data for M1-like macrophages obtained from six different donors in the presence or absence of 10 μM PSB603. Each symbol represents one donor and the lines show mean ± S.E.M. of the median fluorescence intensities (MFI). (C) Flow cytometry histograms obtained in the absence and presence of PSB603 in a representative experiment from M2-like macrophages prepared from monocytes from a single donor (matched with the M1-like data a-b). (D) Mean data for M2-like macrophages obtained from six different donors in the presence or absence of 10 μM PSB603. Each symbol represents one donor and the lines show mean ± S.E.M. of the MFIs. **$p<.01$ paired t-test. (E) Specific binding (MFI, mean fluorescence intensity) of PSB603-BY630 to M1-like and M2-like macrophages derived from the same donor. Specific binding was taken as the difference in MFI between total binding and that obtained in the presence of 10 μM PSB603 for each donor (taken from (B) and (D).

way to monitoring the endogenous expression levels of these two important adenosine receptors on immune cells. PSB603-BY630 bound with high affinity (18.3 nM) to NLuc-tagged A_{2B}Rs stably expressed in HEK293G cells. The ligand exhibited very high selectivity for the A_{2B}R with negligible specific-binding detected to NLuc-A_{2A}R, NLuc-A_1R or NLuc-A_3R receptors at concentrations up to 500 nM. Competition binding studies demonstrated the expected pharmacology at A_{2B}R with the A_{2B}R-selective ligands PSB603[4,32] and MRS-1706[44] demonstrating potent inhibition of the specific binding of 50 nM PSB603-BY630. In contrast, selective A_{2A}R-antagonists SCH442416 and SCH58261,[45,46] The A_1R-selective antagonist SLV320[34] and the A_3R selective antagonist MRS1220[33] were much lower affinity. Finally, kinetic studies undertaken at 37°C showed that equilibrium was reached within 60 min with 200 nM PSB603-BY630 and analysis of the dissociation of the fluorescent ligand, initiated by addition of 10 μM MRS-1706, allowed the residence time of PSB603-BY630 to be determined as 15.4 min.

To establish whether the fluorescent variant of PSB603 still behaved as an A_{2B}R antagonist in functional studies, we took advantage of the highly sensitive GloSensor biosensor for cAMP which is expressed in HEK293G cells and allows monitoring of functional responses mediated by A_{2B}R and A_{2A}R which are both endogenously expressed in these cells.[4] Using the highly selective A_{2B}-selective agonist BAY 60–6583, we showed that PSB603-BY630 was able to inhibit functional response to the A_{2B}R-selective agonist in HEK293G cells endogenously expressing A_{2B}R. However, a striking feature of the antagonism produced by PSB603-BY630 was that the main effect was a reduction of the maximal response to BAY 60–6583 with no significant effect on the agonist EC_{50} value. These data suggest a non-competitive action of PSB603-BY630. Furthermore, in a stable HEK293G cell line overexpressing recombinant human NLuc-A_{2B}Rs, the EC_{50} values for BAY 60–6583 were shifted to lower agonist concentrations consistent with an increase in the spare receptor reserve caused by A_{2B}R overexpression. In these cells PSB603-BY630 did produce a small increase in the EC_{50} for BAY 60–6583 but this was accompanied by a significant decrease in the maximal response to BAY 60–6583, again consistent with a non-competitive interaction with BAY 60–6583 at the A_{2B}R.

We have previously observed a similar non-competitive effect of the parent compound PSB603 on BAY 60-6583-mediated GloSensor responses in HEK293G cells which was consistent with a negative allosteric effect of PSB603 at the A_{2B}R.[4] These data are consistent with a recent A_{2B}R-BAY60-6583-G_s cryo-EM structure that revealed an orthosteric binding pocket for BAY60-6583 that was similar to that of NECA, but with a secondary binding pocket extending out from the orthosteric binding site where residues $V250^{6.51}$ and $N273^{7.36}$ appear to be key determinants of its selectivity for A_{2B}R.[14] These data suggest that PSB603-BY630 may also act as a negative allosteric regulator of the A_{2B}R when coupled to Gs-mediated responses.

A major driver for the generation of a selective red-emitting fluorescent ligand for the A_{2B}R was the need for a tool compound that could be used to monitor surface A_{2B}R expression in individual immune cells. Recent studies have suggested that A_{2B}Rs may regulate the immune response to the tumor microenvironment,[20–22] in addition to the well-established role of A_{2A}Rs on immune cells in relation to cancer progression.[15–19] As a first step towards this, we have used flow cytometry to monitor specific PSB603-BY630 binding to A_{2B}Rs on M1-like and M2-like human macrophages prepared from CD14+ monocytes from six different healthy donors. The data obtained show that this ligand can be used to detect endogenous A_{2B}R expression in M1- and M2-like macrophages. Given that individual cells will contain both specific (A_{2B}R) and non-specific binding sites, we chose to use median fluorescence intensity (MFI) to monitor the extent of A_{2B}R receptor-specific binding. Using this approach there was a significant ($p < 0.01$; paired t-test) reduction in the total binding MFI measured with 100 nM PSB603-BY630 in each donor in macrophages pre-treated with 10 μM PSB603.

In summary, the present manuscript reports on the pharmacological properties of a new red-emitting fluorescent ligand for the A_{2B}R that has high affinity and selectivity. Furthermore, studies on M1- and M2-like macrophages derived from CD14+ human monocytes have confirmed that PSB603-BY630 can be used to monitor the endogenous expression of A_{2B}R on immune cells. This ligand is an important addition to the library of fluorescent ligands, which are selective for each of the adenosine receptor subtypes, and should enhance the study of the role of adenosine receptors on immune cells in the tumor microenvironment.

AUTHOR CONTRIBUTIONS

Participated in research design: HF, LEK, BK, SJH. Conducted experiments: FP, SJM, NDK, EC, JG. Performed data analysis: FP, SJH. Wrote or contributed to the writing of the manuscript: all authors.

ACKNOWLEDGMENTS

This work was supported by the Medical Research Council (grant number MR/W016176/1). FP was supported by a BBSRC studentship (grant number BB/T0083690/1). LEK was supported by a University of Nottingham Anne McLaren Fellowship. Development of PSB603-BY630 was funded by CRUK clinical post-doctoral bursary awarded to HF (grant number C50808/A24952) whilst HF was supported by an NIHR Academic Clinical Lectureship in Medical Oncology.

CONFLICT OF INTEREST STATEMENT

The authors declare no conflicts of interest.

DATA AVAILABILITY STATEMENT

The data that support the findings of this study are available from the corresponding author upon reasonable request.

ETHICS STATEMENT

Heparinised whole blood was obtained by venepuncture from the antecubital fossa of the arm of healthy volunteers after written

informed consent (Ethics from University of Nottingham Ethics committee, ref 161–1711).

ORCID

Foteini Patera https://orcid.org/0000-0001-6997-8865
Sarah J. Mistry https://orcid.org/0000-0003-1409-0097
Eleonora Comeo https://orcid.org/0000-0001-5339-5382
Joelle Goulding https://orcid.org/0000-0002-6227-4483
Barrie Kellam https://orcid.org/0000-0003-0030-9908
Laura E. Kilpatrick https://orcid.org/0000-0001-6331-5606
Hester Franks https://orcid.org/0000-0001-5378-6076
Stephen J. Hill https://orcid.org/0000-0002-4424-239X

REFERENCES

1. Fredholm BB, IJzerman AP, Jacobson KA, Linden J, Müller CE. International Union of Basic and Clinical Pharmacology. LXXXI. Nomenclature and classification of adenosine receptors-an update. *Pharmacol Rev*. 2011;63(1):1-34. doi:10.1124/pr.110.003285
2. Borea PA, Gessi S, Merighi S, Vincenzi F, Varani K. Pharmacology of adenosine receptors: the state of the art. *Physiol Rev*. 2018;98(3):1591-1625.
3. Müller CE, Jacobson KA. Recent developments in adenosine receptor ligands and their potential as novel drugs. *Biochim Biophys Acta*. 2011;1808(5):1290-1308.
4. Goulding J, May LT, Hill SJ. Characterisation of endogenous A_{2A} and A_{2B} receptor-mediated cyclic AMP responses in HEK 293 cells using the GloSensor™ biosensor: evidence for an allosteric mechanism of action for the A_{2B}-selective antagonist PSB 603. *Biochem Pharmacol*. 2018;147:55-66.
5. Hinz S, Lacher SK, Seibt BF, Müller CE. BAY60-6583 acts as a partial agonist at adenosine A2B receptors. *J Pharmacol Exp Ther*. 2014;349(3):427-436.
6. Gao ZG, Inoue A, Jacobson KA. On the G protein-coupling selectivity of the native A_{2B} adenosine receptor. *Biochem Pharmacol*. 2018;151:201-213.
7. Linden J, Thai T, Figler H, Jin X, Robeva AS. Characterization of human a(2B) adenosine receptors: radioligand binding, western blotting, and coupling to G(q) in human embryonic kidney 293 cells and HMC-1 mast cells. *Mol Pharmacol*. 1999;56(4):705-713.
8. Voss JH, Mahardhika AB, Inoue A, Müller CE. Agonist-dependent coupling of the promiscuous adenosine A_{2B} receptor to Gα protein subunits. *ACS Pharmacol Transl Sci*. 2022;5(5):373-386.
9. Jaakola VP, Griffith MT, Hanson MA, et al. The 2.6 angstrom crystal structure of a human A2A adenosine receptor bound to an antagonist. *Science*. 2008;322(5905):1211-1217.
10. Lebon G, Warne T, Edwards PC, et al. Agonist-bound adenosine A2A receptor structures reveal common features of GPCR activation. *Nature*. 2011;474(7352):521-525.
11. Xu F, Wu H, Katritch V, et al. Structure of an agonist-bound human A2A adenosine receptor. *Science*. 2011;332(6027):322-327.
12. García-Nafría J, Lee Y, Bai X, Carpenter B, Tate CG. Cryo-EM structure of the adenosine A_{2A} receptor coupled to an engineered heterotrimeric G protein. *elife*. 2018;4(7):e35946.
13. Thimm D, Schiedel AC, Sherbiny FF, et al. Ligand-specific binding and activation of the human adenosine a(2B) receptor. *Biochemistry*. 2013;52(4):726-740.
14. Chen Y, Zhang J, Weng Y, et al. Cryo-EM structure of the human adenosine A_{2B} receptor-G_s signaling complex. *Sci Adv*. 2022;8(51):eadd3709.
15. Ohta A, Gorelik E, Prasad SJ, et al. A2A adenosine receptor protects tumors from antitumor T cells. *Proc Natl Acad Sci USA*. 2006;103(35):13132-13137.
16. Ohta A. A metabolic immune checkpoint: adenosine inTumor microenvironment. *Front Immunol*. 2016;7:109.
17. Inoue Y, Yoshimura K, Kurabe N, et al. Prognostic impact of CD73 and A2A adenosine receptor expression in non-small-cell lung cancer. *Oncotarget*. 2017;8:8738-8751.
18. Zhang C, Wang K, Wang H. Adenosine in cancer immunotherapy: taking off on a new plane. *Biochim Biophys Acta Rev Cancer*. 2023;1878(6):189005.
19. Yu F, Zhu C, Xie Q, Wang Y. Adenosine A_{2A} receptor antagonists for cancer immunotherapy. *J Med Chem*. 2020;63(21):12196-12212.
20. Evans JV, Suman S, Goruganthu MUL, et al. Improving combination therapies: targeting A2B-adenosine receptor to modulate metabolic tumor microenvironment and immunosuppression. *J Natl Cancer Inst*. 2023;115(11):1404-1419.
21. Strickland LN, Faraoni EY, Ruan W, Yuan X, Eltzschig HK, Bailey-Lundberg JM. The resurgence of the Adora2b receptor as an immunotherapeutic target in pancreatic cancer. *Front Immunol*. 2023;28(14):1163585.
22. Dutta S, Ganguly A, Chatterjee K, Spada S, Mukherjee S. Targets of immune escape mechanisms in cancer: basis for development and evolution of cancer immune checkpoint inhibitors. *Biology (Basel)*. 2023;12(2):218.
23. Ludwig N, Yerneni SS, Azambuja JH, et al. Tumor-derived exosomes promote angiogenesis via adenosine A_{2B} receptor signaling. *Angiogenesis*. 2020;23(4):599-610.
24. Hill SJ, Kilpatrick LE. Kinetic analysis of fluorescent ligand binding to cell surface receptors: insights into conformational changes and allosterism in living cells. *Br J Pharmacol*. 2023.
25. Goulding J, Kondrashov A, Mistry SJ, et al. The use of fluorescence correlation spectroscopy to monitor cell surface β2-adrenoceptors at low expression levels in human embryonic stem cell-derived cardiomyocytes and fibroblasts. *FASEB J*. 2021;35(4):e21398.
26. Lay CS, Isidro-Llobet A, Kilpatrick LE, Craggs PD, Hill SJ. Characterisation of IL-23 receptor antagonists and disease relevant mutants using fluorescent probes. *Nat Commun*. 2023;14(1):2882.
27. White CW, Caspar B, Vanyai HK, Pfleger KDG, Hill SJ. CRISPR-mediated protein tagging with Nanoluciferase to investigate native chemokine receptor function and conformational changes. *Cell Chem Biol*. 2020;27(5):499-510.e7.
28. Comeo E, Kindon ND, Soave M, et al. Subtype-selective fluorescent ligands as pharmacological research tools for the human adenosine A_{2A} receptor. *J Med Chem*. 2020;63(5):2656-2672.
29. Stoddart LA, Kindon ND, Otun O, et al. Ligand-directed covalent labelling of a GPCR with a fluorescent tag in live cells. *Commun Biol*. 2020;3(1):722.
30. Neustadt BR, Hao J, Lindo N, et al. Potent, selective, and orally active adenosine A2Areceptor antagonists: Arylpiperazine derivatives of Pyrazolo[4,3-e]-1,2,4-Triazolo[1,5-c]pyrimidines. *Bioorg Med Chem Lett*. 2007;17(5):1376-1380.
31. Köse M, Gollos S, Karcz T, et al. Fluorescent-labeled selective adenosine A_{2B} receptor antagonist enables competition binding assay by flow cytometry. *J Med Chem*. 2018;61(10):4301-4316.
32. Borrmann T, Hinz S, Bertarelli DC, et al. 1-alkyl-8-(piperazine-1-sulfonyl)phenylxanthines: development and characterization of adenosine A2B receptor antagonists and a new radioligand with subnanomolar affinity and subtype specificity. *J Med Chem*. 2009;52(13):3994-4006.
33. Vernall AJ, Stoddart LA, Briddon SJ, Hill SJ, Kellam B. Highly potent and selective fluorescent antagonists of the human adenosine a_3 receptor based on the 1,2,4-triazolo[4,3-a]quinoxalin-1-one scaffold. *J Med Chem*. 2012;55:1771-1782.
34. Comeo E, Trinh P, Nguyen AT, et al. Development and application of subtype-selective fluorescent antagonists for the study of the human adenosine A_1Receptor in living cells. *J Med Chem*. 2021;64(10):6670-6695.

35. Fan F, Binkowski BF, Butler BL, Stecha PF, Lewis MK, Wood KV. Novel genetically encoded biosensors using firefly luciferase. *ACS Chem Biol*. 2008;3:346-351.
36. Stoddart LA, Johnstone EKM, Wheal AJ, et al. Application of BRET to monitor ligand binding to GPCRs. *Nat Methods*. 2015;12(7):661-663.
37. Cooper SL, Wragg ES, Pannucci P, Soave M, Hill SJ, Woolard J. Regionally selective cardiovascular responses to adenosine A_{2A} and A_{2B} receptor activation. *FASEB J*. 2022;36(4):e22214.
38. Balaji J, Ryan TA. Single-vesicle imaging reveals that synaptic vesicle exocytosis and endocytosis are coupled by a single stochastic mode. *Proc Natl Acad Sci USA*. 2007;104:20576-20581.
39. Harding SD, Sharman JL, Faccenda E, et al. The IUPHAR/BPS guide to pharmacology in 2019: updates and expansion to encompass the new guide to immunopharmacology. *Nucleic Acids Res*. 2018; 46:D1091-D1106.
40. Alexander SPH, Christopoulos A, Davenport AP, et al. The concise guide to pharmacology 2019/20: g protein-coupled receptors. *Br J Pharmacol*. 2019;176(1):S21-S141.
41. Baker JG, Middleton R, Adams L, et al. Influence of fluorophore and linker composition on the pharmacology of fluorescent adenosine A1 receptor ligands. *Br J Pharmacol*. 2010;159(4):772-786.
42. Kok ZY, Stoddart LA, Mistry SJ, et al. Optimization of peptide linker-based fluorescent ligands for the histamine H_1 receptor. *J Med Chem*. 2022;65(12):8258-8288.
43. Jiang J, Seel CJ, Temirak A, et al. A_{2B} adenosine receptor antagonists with Picomolar potency. *J Med Chem*. 2019;62(8):4032-4055.
44. Trincavelli ML, Marroni M, Tuscano D, et al. Regulation of A2B adenosine receptor functioning by tumour necrosis factor a in human astroglial cells. *J Neurochem*. 2004;91(5):1180-1190.
45. Ongini E, Dionisotti S, Gessi S, Irenius E, Fredholm BB. Comparison of CGS15943, ZM 241385 and SCH 58261 as antagonists at human adenosine receptors. *Naunyn Schmiedeberg's Arch Pharmacol*. 1999;359:7-10.
46. Moresco RM, Todde S, Belloli S, et al. In vivo imaging of adenosine A2A receptors in rat and primate brain using [11C]SCH442416. *Eur J Nucl Med Mol Imaging*. 2005;32(4):405-413.

SUPPORTING INFORMATION

Additional supporting information can be found online in the Supporting Information section at the end of this article.

How to cite this article: Patera F, Mistry SJ, Kindon ND, et al. A novel and selective fluorescent ligand for the study of adenosine A_{2B} receptors. *Pharmacol Res Perspect*. 2024;12:e1223. doi:10.1002/prp2.1223